HHS Public Access

Author manuscript

Mol Cancer Ther. Author manuscript; available in PMC 2019 December 01.

Published in final edited form as:

Mol Cancer Ther. 2018 December ; 17(12): 2689–2701. doi:10.1158/1535-7163.MCT-18-0399.

ST8SIA1 regulates tumor growth and metastasis in TNBC by activating the FAK-AKT-mTOR signaling pathway

Khoa Nguyen[#1], **Yuanqing Yan**[#2], **Bin Yuan**[1], **Abhishek Dasgupta**[1], **Jeffrey Sun**[1], **Hong Mu**[1], **Kim-Anh Do**[2], **Naoto T. Ueno**[3], **Michael Andreeff**[1,#], and **V. Lokesh Battula**[1,3,#]

[1]Department of Leukemia, Section of Molecular Hematology and Therapy, Department of Leukemia

[2]Department of Biostatistics, The University of Texas MD Anderson Cancer Center, Houston, Texas, USA

[3]Section of Translational Breast Cancer Research, Department of Breast Medical Oncology, The University of Texas MD Anderson Cancer Center, Houston, Texas, USA.

[#] These authors contributed equally to this work.

Abstract

Breast cancer stem-like cells (BCSCs) are implicated in cancer recurrence and metastasis of triple negative breast cancer (TNBC). We have recently discovered that ganglioside GD2 expression defines BCSCs and that ST8SIA1 regulates GD2 expression and BCSC function. In this report, we show that ST8SIA1 is highly expressed in primary TNBC; its expression is positively correlated with the expression of several BCSC associated genes such as BCL11A, FOXC1, CXCR4, PDGFRβ, SOX2 and mutations in p53. CRISPR knockout of ST8SIA1 completely inhibited BCSC functions, including *in vitro* tumorigenesis and mammosphere formation. Mechanistic studies discovered activation of the FAK-AKT-mTOR signaling pathway in $GD2^+$ BCSCs, and its tight regulation by ST8SIA1. Finally, knockout of ST8SIA1 completely blocked *in vivo* tumor growth and metastasis by TNBC cells. In summary, this data demonstrates the mechanism by which ST8SIA1 regulates tumor growth and metastasis in TNBC and identifies it as a novel therapeutic target.

Keywords

Breast cancer stem cells; GD2; Triple negative breast cancer; ST8SIA1; FAK-AKT-mTOR signaling

[#]**Corresponding Authors:** Michael Andreeff and V. Lokesh Battula, Department of Leukemia,. The University of Texas MD Anderson Cancer Center, 1515 Holcombe Blvd., Unit 448, Houston, TX 77030 USA, Phone: 713-792-7261, Fax: 713-563-7355, mandreef@mdanderson.org and vbattula@mdanderson.org.

Conflicts of Interest: Authors have no conflicts of interest to disclose.

Introduction

Breast cancer stem-like cells (BCSCs) comprise a small proportion of cells present in primary or metastatic breast tumors, but they are strongly tumorigenic, quiescent, chemoresistant, highly metastatic and promote tumor relapse (1–3). To successfully develop BCSC-targeted therapy, molecular markers that are specific to BCSCs must be identified. Several cell surface and intracellular markers have been discovered to prospectively isolate BCSCs from primary breast tumors and the $CD44^{high}CD24^{low}$ phenotype was reported to be specific for BCSCs (4). In addition, aldehyde dehydrogenase enzyme activity has been shown to distinguish BCSCs within primary breast tumors (5). We have recently identified the ganglioside GD2 as a single cell surface marker characterizing BCSCs in cell lines and primary tumors (6). GD2 is co-expressed on the $CD44^{high}CD24^{low}$ fraction of breast cancer cells and its expression has been shown to be higher in basal-like breast cancer cell lines than in their luminal counterparts (6). $GD2^+$ cells are highly tumorigenic *in vivo*; as few as ten $GD2^+$ cells can initiate tumors in NOD/SCID mice.

GD2 is synthesized by GD2 synthase (B4GALNT1) with GD3 as precursor, whereas GD3 is synthesized by GD3 synthase (ST8SIA1) with GM3 as precursor. Using gene expression arrays, we found that ST8SIA1 but not B4GALNT1 is highly expressed in $GD2^+$ BCSCs. These findings were confirmed by other groups, which also found upregulation of ST8SIA1 in BCSCs (7, 8). While GD2 has been shown to be highly expressed in basal-like breast cancer cell lines compared to their luminal counterparts, expression levels of ST8SIA1 in other breast cancer subtypes have not been studied. We have previously shown that knockdown of ST8SIA1 inhibited BCSC function, including anchorage-independent growth, migration, and invasion (6). In addition, induction of epithelial-to-mesenchymal transition (EMT), which induced the $CD44^{high}CD24^{low}$ BCSC phenotype, also induced ST8SIA1 expression in breast cancer cells (6). Moreover, ST8SIA1 overexpression in breast cancer cell lines in turn induced EMT and metastasis *in vivo* (9). We very recently showed that ST8SIA1 expression is regulated by NFκB signaling (10). Inhibition of NFκB activation subunits such as IKKα/β inhibited ST8SIA1 expression and BCSC function *in vitro* and inhibited tumor growth and metastasis *in vivo*. However, the mechanism underlying ST8SIA1 knockdown-mediated tumor growth inhibition is unknown.

Focal adhesion kinase (FAK) signaling has been well characterized for its role in cell adhesion, migration, and metastasis (11). Inhibition of FAK signaling hinders migration and invasion of cancer cells. However, the molecular interactions between GD2 and FAK in the regulation of BCSC function including tumor initiation and metastasis have not been investigated. GD2 has been shown to bind cell surface receptors, including integrins, in the extracellular matrix and to activate downstream FAK signaling in cancer cells (12, 13). GD2 acts as a co-receptor for other cell surface receptors, including cMet and EGFR, to activate downstream signaling (8, 14). FAK regulates cellular activities including cell survival, adhesion, proliferation, and migration by activating several signal transducers, including PI3K, AKT, mTOR, RAS, and ERK/MAPK (15–20). These proteins further activate their downstream target genes to regulate cellular functions.

The purpose of this study was to determine the expression of ST8SIA1 in TNBC and its role in the progression of these cancers. Our results show that ST8SIA1 is highly upregulated in basal-like TNBC primary tumors and regulates breast tumor growth and metastasis. We also found signaling pathways that are highly activated in $GD2^+$ BCSCs and that these signaling events are dependent on ST8SIA1 expression.

Materials and Methods

Cell Culture

Human breast cancer cell lines SKBR3, ZR75–1, MDA361, BT474, MCF7, MDA453, T47D, SUM149, HCC38, MDA468, MDA-MB-231, SUM159, and HS578T were cultured in complete cell culture medium comprising Dulbecco modified essential medium (DMEM) containing 10% fetal bovine serum (FBS) and 1% penicillin and streptomycin with glutamine. Cells were routinely checked for mycoplasma using the PCR Mycoplasma Detection Kit (Applied Biological Materials; Richmond, BC, Canada). All the cell lines are fingerprinted routinely every six months at cell line core facility at MD Anderson for purity.

Flow Cytometry Analysis and Fluorescence-activated Cell Sorting

Flow cytometry staining of MDA-MB-231, SUM159, and their respective ST8SIA1-knockout (KO) cells was performed using a previously described method (6). In summary, cells ($\sim 1\times10^6$) were incubated with allophycocyanin (APC)-conjugated anti-GD2 antibody (BioLegend; San Diego, CA) for 30 minutes on ice in the dark. For measuring the expression of ceramide, GM1 and GM3 the cells were stained using anti-ceramide (Enzo Life Sciences, Farmingdale, NY) or anti-GM1 (Abcam, Cambridge, MA) or anti-GM3 (Cosmo Bio USA, Carlsbad, CA) unconjugated antibodies. After washes, the cells were incubated with APC conjugated anti-mouse or anti-rabbit IgG secondary antibody. The cells were washed once with FACS buffer containing 4′, 6-diamino-2-phenylindole (DAPI; 1 μg/mL). The cells were analyzed by an LSR II (BD; Franklin Lakes, NJ) or Galios (Beckman Coulter; Brea, CA) flow cytometers. Cell sorting was performed on the FACSAria II (BD) as described before(10).

Generation of ST8SIA1-knockout cells using CRISPR-Cas9 approach

A specially designed gRNA targeting the ST8SIA1 gene was developed and purchased from (GenScript Biotechnologies; Piscataway, NJ). The sequence of the gRNA is underlined in Supplementary Figure 3. To generate the ST8SIA1-KO cells, SUM159 and MDA-MB-231 cells were transfected with 1 μg of gRNA specific to ST8SIA1 and 1 μg of Cas9 plasmid (Systems Biosciences, Palo Alto, CA) using jetPRIME transfection reagent (Polyplus; New York, NY). After 72hrs of transfection the cells FACS sorted into 96-well plates (one cell per well) to generate homogenous KO colonies. Colonies were expanded and analyzed for GD2 expression by flow cytometry.

Sanger DNA Sequencing

Low passage Cas9-Control and ST8SIA1-KO (below 5) were cultured in standard media. Once confluent, 3×10^6 cells were trypsinized and pelleted for processing. DNA was then extracted using DNEasy kit from Qiagen (Hilden, Germany). The gene of interest was then

amplified using the ThermoFisher Scientific PlatinumTaq DNA Polymerase kit (Waltham, MA) along with custom designed forward and reverse primers (from 5' to 3' respectively, TGT GGT ATG ACG GGG AGT TT and ACC TTT GCC GAA TTA TGC TG)(Integrated DNA Technologies; Coralville, IA) and purified through gel electrophoresis. DNA samples of Cas9-Control and ST8SIA1-KO cells were then sequenced by Sanger-sequencing at MD Anderson Sequencing Core facility.

RT-PCR

RT-PCR was performed using the TaqMan gene expression assay from Applied Biosystems (Carlsbad, CA) as previously described (10). The primers used were as follows: GAPDH: Hs002758991_g1, B2M: Hs00187842_m1, ST8SIA1: Hs00268157_m1, BCL11A: Hs01093197_m1, PDGFRß: Hs01019589_m1, VCAM1: Hs01003372_m1, PDGFRα: Hs00998026_m1, DKK1: Hs00183740_m1, SOX2: Hs01053049_s1, FOXG1: Hs01850784_s1, CXCR4: Hs00607978_s1, CXCL12: Hs03676656_mH, and FGFR2: Hs01552926_m1. Relative mRNA expression was normalized to GAPDH.

Proteomics Analysis

To investigate signaling pathways that are activated in BCSCs, $GD2^+$ and $GD2^-$ SUM159 cells were subjected to FACS and then to proteomic profiling by Kinexus antibody array analysis (Vancouver, BC, Canada). Lysates of $GD2^+$ and $GD2^-$ cells were labeled with fluorescent probes and applied to glass slides coated with 850 validated antibodies against various total and phosphorylated proteins per the manufacturer's instructions. After washes, the stain was developed and analyzed on a phosphoimager. The z-ratio was calculated as previous described(10) and proteins differentially expressed or phosphorylated between $GD2^+$ and $GD2^-$ cells were identified.

Western Blotting

Protein lysates were prepared by pelleting cells (3×10^6) and subjecting them to lysis using 200 μL of Mammalian Cell Lysis Buffer (G-Biosciences; St. Louis, MO) and 1 μL of protease and phosphatase inhibitor Cocktail (Roche Diagnostics; Basel, Switzerland). The lysates were subjected to polyacrylamide gel electrophoresis and then transferred to PVDF membrane. The membranes were then blocked with 5% milk and incubated with primary (listed in Supplementary Table 3) and fluorescent tagged secondary antibodies. After washes the membranes scanned using Odyssey fluorescent imager/scanner (LI-COR).

Mammosphere Assay

Cas9-Control or ST8SIA1-KO MDA-MB-231 and SUM159 cells were plated at 1×10^3 per well in ultra-low attachment 24-well plates (Corning; Corning, NY) containing I ml per well mammosphere growth medium (Promocell; Heidelberg, Germany). To test the effect of FAK and mTOR signaling inhibition on mammosphere formation, MDA-MB-231 and SUM159 cells were treated with PF-573228 (Sigma, Ronkonkoma, NY) or everolimus (Chemscene, Monmouth Junction, NJ). The mammospheres were stained and counted as described before(10). PF-573228 structure and method of use was previously described in the report from Slack-Davis JK et al.(21).

In Vitro Tumorigenesis Assay

In vitro analysis tumorigenesis potential was determined by soft-agar colony assay. ST8SIA1-KO and Cas9 control SUM159 and MDA-MB-231 cells or cells treated with FAK an mTOR inhibitors were used for this assay. Five × 10^3 cells per well were cultured in complete cell culture medium containing 1% and 0.5% low-melting agarose in a dual layer setting. The cells were cultured at 37°C with 5% CO_2 for 3 weeks. The colonies were stained and imaged as described before(10).

Migration Assay

Migration assays were performed using 24-well transwell chambers, using membrane inserts with 8-μm pores (Corning; Kennebunk, ME) as described before(10). Briefly, Cas9-Control and ST8SIA1-KO SUM159 or MDA-MB-231 cells in DMEM containing 1% FBS were seeded (1×10^4 per chamber) into the upper chambers. After incubating for 8 hours at 37°C in a 5%CO_2 incubator, each membrane was carefully removed from the insert, fixed with 2% formalin, and stained with DAPI. Fluorescent images were captured using the EVOS automated microscope (Thermo Fisher Scientific).

In Vivo Tumor Growth

All experiments involving animals were approved by and conducted in accordance with the policies of the Institutional Animal Care and Use Committee (IACUC) of The University of Texas MD Anderson Cancer Center. Three × 10^6 viable Cas9-Control or ST8SIA1-KO cells were resuspended in ECMatrix solution (EMD Millipore; Billerica, MA) and implanted into the mammary fat pads NSG mice (n=20; 10 mice per group). Tumor volumes were measured weekly by using calipers. When the tumors reach 2 cm in diameter, the animal was humanely euthanized per IACUC guidelines. The animal survival curves were generated by log-rank test. After euthanasia, the tumors were harvested from both groups for immunohistochemical (IHC) studies.

In Vivo Metastasis

Cas9-Control and ST8SIA1-KO MDA-MB-231 cells were subjected to trypsinization and suspended in PBS (5×10^6 cells/mL). NSG mice were injected with cells (5×10^5 in 100 μL volume per mouse) via tail vein (n=18; 9 mice per group). Beginning in week 3, three mice randomly selected from each group were sacrificed weekly; body organs, including lungs, liver, and femur, were isolated and subjected to histologic analysis with hematoxylin and eosin (H&E) staining. The slides were then scanned on the EVOS automated microscope (Invitrogen).

Statistical Analysis

Unless otherwise indicated, data shown represent the mean and ± standard error of the mean.

TCGA Data Analysis.—A total of 1093 breast cancer samples with 112 normal matched tissues were investigated. Of the breast cancer samples, 109 were identified as TNBC from the clinical information provided. Based on PAM50 classification, another 232 were Luminal A, 129 Luminal B, 98 Basal, and 58 HER2. The data for these breast cancer

subtypes also were analyzed. RNAseq data were quantile-normalized to remove the sample variability and any potential batch effects. Differential expression of ST8SIA1 between groups was identified by using the Student *t*-test or ANOVA with Tukey's HSD post hoc test in the R software (version 3.2.0). Differential expression of ST8SIA1 in mutated genes vs non-mutated genes was tested by the Student *t*-test and the resulting p-values and fold-changes are reported.

RNAseq Analysis.—Samples were sequenced on the HiSeq Sequencing System by the Sequencing and Microarray Core facility at MD Anderson. Sequence reads were mapped to human genomics (build hg19) with bowtie2 aligner using RSEM software (22, 23). The EdgeR package in R was used to compare the differential expression between ST8SIA1-KO samples and controls (24). Genes with adjusted p-values less than 0.05 and absolute fold-changes larger than 2 were considered significant. To investigate the relationships between ST8SIA1 and the significant genes identified from our KO experiment, we used the Pearson correlation in the breast cancer expression data obtained from TCGA. A scatterplot with $\log_2$ fold-change from expression in KO and TCGA correlation coefficients was plotted.

Results

ST8SIA1 expression is associated with basal-like TNBC tumor phenotype

Development of ST8SIA1-targeted therapy for breast cancer necessitates investigation of ST8SIA1 expression in different breast cancer subtypes. To investigate the expression of ST8SIA1 in primary breast tumors, we analyzed RNAseq data from over 1100 primary and metastatic breast tumors and adjacent normal tissues from the TCGA database and found that ST8SIA1 was overexpressed in about 11% of these breast cancers (Fig 1A). Interestingly, the estrogen receptor (ER)-negative and progesterone receptor (PR)–negative phenotype in these breast tumors was highly correlated with ST8SIA1 overexpression ($p<0.001$ for both ER and PR), whereas HER2 overexpression was not (Fig 1A). Basal-type tumors expressed the highest levels of ST8SIA1 of all other types, including Luminal A, Luminal B, or HER2-enriched tumors (all $p=0.001$; Fig 1B). Moreover, primary TNBC tumors (n=115) had 4.63-fold higher expression levels of ST8SIA1 than non-TNBC tumors (n=852, $p<0.001$; Fig 1C). A survival analysis by the log-rank test indicated that patients with $ST8SIA1^{high}$ tumors had significantly lower rates of disease-free (p=0.0109; Fig 1D) and overall (p=0.0148; Fig 1E) survival than patients with $ST8SIA1^{low}$ tumors. Indeed, in cell lines, we validated these findings in luminal or basal cell–derived breast cancer cell lines (n=10) and found that ST8SIA1 expression was, on average, 50-fold higher in basal subtype breast cancer cell lines than in luminal subtypes (Supplementary Figure 1). These data suggest that ST8SIA1 expression is associated with the basal-like and TNBC tumors and that high levels of ST8SIA1 in tumors may lead to shorter survival in breast cancer patients.

ST8SIA1 expression is associated with mutations in TP53 gene and positively correlated with expression of genes associated with the stem cell phenotype

To investigate the relationships between ST8SIA1 expression and genes frequently mutated in breast cancer, the top 20 most frequent mutations in the TCGA breast cancer data set were analyzed for correlation with ST8SIA1 mRNA expression (Fig 2A). Of these 20 genes,

TP53 had the strongest positive correlation with ST8SIA1 expression ($p<0.00001$); ST8SIA1 expression was >2-fold higher in TP53-mutated than in TP53–wild type tumors (Fig 2B). Another positively correlated mutation was for the nuclear envelope protein Spectrin Repeat Containing Nuclear Envelope 1 (SYNE1; $p<0.05$; Fig 2B). On the other end of the spectrum, GATA3 mutations were the most negatively correlated ($p<0.001$) with ST8SIA1 expression (Fig 2B). GATA3 plays a role in epithelial cell differentiation in the mammary gland and is a major tumor suppressor, supporting the notion that ST8SIA1 is a stem cell–associated gene.

To identify the genes that are co-expressed with ST8SIA1, we analyzed TCGA data in the breast cancer data set. Pearson correlation coefficients (Pearson's r) > 0.5 were considered positively correlated, while those with Pearson's $r < -0.5$ were considered negative correlated. We found that 139 genes were positively and 108 genes negatively correlated with ST8SIA1 (Supplementary Figure 2). Among these genes, those associated with BCSC function include BCL11A (25) (Pearson's $r = 0.645$) and FOXC1 (26, 27) (Pearson's $r = 0.61$), both of which were highly positively correlated with ST8SIA1 expression (Fig 2C). In addition, tumor suppressor gene GATA3 (28) (Pearson's $r = -0.583$) and its closely associated protein FOXA1 (29) (Pearson's $r = -0.615$) were highly negatively correlated with ST8SIA1 (Fig 2C). These data suggest that ST8SIA1 has a strong positive correlation with p53 mutations but a negative correlation with GATA3 mutations. Finally, we found that ST8SIA1 expression was positively correlated with genes that promote tumor growth and negatively associated with genes that inhibit tumor growth.

Knockout of ST8SIA1 completely blocks GD2 expression and inhibits cancer stem cell function in TNBC cells

To further investigate the mechanism of ST8SIA1-mediated regulation of BCSC function, we used a CRISPR/Cas9 gene KO approach to generate ST8SIA1-KO SUM159 and MDA-MB-231 TNBC cells. DNA sequencing of SUM159 and MDA-MB-231 cDNA identified a single nucleotide insertion into exon 3 of the ST8SIA1 gene (Supplementary Figure 3A&B). To validate that KO of ST8SIA1 was successful, GD2 expression of ST8SIA1-KO SUM159 and MDA-MB-231 cells was analyzed by flow cytometry and was <1% for both SUM159 and MDA-MB-231 KO cells, while it was 17.3% ± 4% and 12.5% ± 3% for their respective Cas9-Control cells (Supplementary Figure 4A&B). Interestingly, knockout of ST8SIA1 induced the cell surface expression of the upstream gangliosides including its substrate GM3 as well as GM1 and ceramide in SUM159 cells (Supplementary figure 4C). This data further demonstrate that knockout of ST8SIA1 completely blocks GD2 expression and therefore upstream gangliosides are accumulated on cell surface. Cell growth analysis in-vitro did not show any significant effects on cell proliferation between control and ST8SIA1-KO cells for the first 10–15 passages (Supplementary Figure 4D).. Therefore, we performed all the in-vitro and in-vivo functional assays involving ST8SIA1-KO cells before they reached passage 10.

To investigate the effects of ST8SIA1 deletion on cancer stem cell activity, Cas9-Control and ST8SIA1-KO SUM159 and MDA-MB-231 cells were subjected to a series of *in vitro* functional assays, including soft-agar colony assays (tumorigenesis), mammosphere

formation assays (anchorage-independent growth), and transwell assays (cell migration). In SUM159 cells, ST8SIA1 KO inhibited *in vitro* tumorigenesis by >30-fold, mammosphere formation by ~10-fold, and cell migration by 2-fold compared to Cas9-Control SUM159 cells (Supplementary Figure 5A). In MDA-MB-231 cells, ST8SIA1 KO inhibited *in vitro* tumorigenesis by 3-fold, mammosphere formation by ~12-fold, and cell migration by 3-fold compared to Cas9-Control MDA-MB-231 cells (Supplementary Figure 5B&C)). These data suggest that inhibition of ST8SIA1 negatively affects BCSC function in TNBC cells.

Genes associated with cancer stem cell properties are positively correlated with ST8SIA1 expression in breast cancer patients and are tightly regulated by ST8SIA1

To better understand the mechanism of ST8SIA1 regulation of BCSC function, we performed RNAseq analysis on ST8SIA1-KO and Cas9-Control SUM159 cells (triplicate samples for both cell types). After setting the parameters to p-value <0.05 and absolute fold-change >2, 1502 genes were found to be downregulated and 842 genes upregulated in ST8SIA1-KO cells compared to Cas9-Control cells (Fig 3A). To investigate the oncogenic signature affected by ST8SIA1 KO, we performed gene set enrichment analysis (GSEA) and found that many major oncogenic pathways, including AKT, EGFR, ERK, Wnt, p53, RB, KRAS, PDGF, and MEK, were downregulated in ST8SIA1-KO cells compared to Cas9-Control cells (Supplementary Table 1). Further, a correlation analysis was performed for genes that were differentially expressed in ST8SIA1-KO cells (x-axis) and genes that were positively or negatively correlated with ST8SIA1 in the TCGA patient data set (y-axis, Fig 3B). Interestingly, 65% of the genes that are positively correlated with ST8SIA1 in TCGA data were also downregulated in ST8SIA1-KO cells (red box, Fig 3B) suggesting that these genes are dependent on ST8SIA1.

To validate the inhibition of gene expression in ST8SIA1-KO cells, we performed qRT-PCR analysis and found that genes that are associated with stem cell functions, including BCL11A, PDGFR-α, PDGFRß, VCAM1, FOXC1, CXCR4, CXCL12, SOX2, FOXG1, FGFR2, and WNT5A, were indeed downregulated in ST8SIA1-KO cells compared to Cas9-Control cells (Fig 3C). DKK1, an antagonist of WNT-ß-Catenin signaling, was upregulated in ST8SIA1-KO cells, suggesting an inhibition of stemness in KO cells (Fig 3C). These data indicate that ST8SIA1 not only is co-expressed with BCSC-associated genes but also regulates their expression, suggesting that targeting ST8SIA1 inhibits BCSC-associated genes in TNBC tumors.

FAK-AKT-ERK-mTOR signaling is highly active in GD2$^+$ BCSCs and this activity is regulated by ST8SIA1

To better define the mechanism by which ST8SIA1 regulates BCSC functions, we performed proteome profiling of GD2$^+$ and GD2$^-$ SUM159 cells. GD2$^+$ and GD2$^-$ SUM159 cells were FACS-sorted (Fig 4A) and the cell lysates were analyzed using Kinexus antibody arrays. Labeled proteins were incubated on glass chips coated with 850 validated antibodies, which were further developed to identify differentially expressed or phosphorylated proteins. After validation for consistency in duplicate samples for each antibody on the chip, the proteins that were differentially upregulated, downregulated, or phosphorylated were identified (listed in Supplementary Table 2). We found that FAK and downstream proteins

associated with this signaling, including Csk, 4E-BP1 (T45 and S65), and STAT3, were upregulated in $GD2^+$ SUM159 cells compared to $GD2^-$ cells. GD2 is known to activate FAK and FAK is known to activate PI3K-AKT-ERK-mTOR signaling. As 4E-BP1 is also activated in $GD2^+$ cells, we hypothesized that FAK-AKT-ERK-mTOR signaling is activated in $GD2^+$ cells.

To test our hypothesis, we performed western blot analysis using antibodies associated with FAK-AKT-ERK-mTOR signaling in lysates of $GD2^+$ and $GD2^-$ SUM159 and MDA-MB-231 cells (Fig 4A). Consistent with the protein antibody array data, we found that FAK (Y861) and 4E-BP1 (S65) were significantly more phosphorylated in $GD2^+$ than in $GD2^-$ cells (Fig 4B). We also found that AKT (S473), ERK (T202/Y204), and mTOR (S2448) were significantly more phosphorylated in $GD2^+$ than in $GD2^-$ SUM159 and MDA231 cells, while total protein levels were relatively unchanged, suggesting that FAK-AKT-ERK-mTOR signaling is activated in $GD2^+$ cells (Fig 4B).

As GD2 expression is regulated by ST8SIA1, we hypothesized that ST8SIA1 regulates cell signaling that is downstream of GD2 in TNBC cells. We analyzed expression and activity of FAK-AKT-ERK-mTOR signaling proteins in ST8SIA1-KO and Cas9-Control SUM159 cells by western blotting and confirmed that pFAK (Y861), pAKT (S473), pERK (T202/Y204), pmTOR (S2448), pStat3, and p4E-BP1 (S65) were downregulated in ST8SIA1-KO cells compared to Cas9-Controls, indicating that FAK-AKT-ERK-mTOR signaling is regulated by ST8SIA1 in BCSCs (Fig 4C).

Targeting FAK or mTOR signaling inhibits BCSC function in TNBC

To investigate the role of FAK-mTOR signaling in BCSC function, *in vitro* tumorigenesis and mammosphere formation (i.e., anchorage-independent growth) was assayed in SUM159 and MDA-MB-231 cells in the presence or absence of FAK inhibitor PF-573228 (Fig 5A) or FDA-approved mTOR inhibitor everolimus (Fig 5B). Soft agar colony formation by both SUM159 and MDA-MB-231 cells was inhibited 5- and 30-fold respectively by PF-573228 in a concentration-dependent manner (1, 10, 100, 1000nM) (Fig 5A) and mammosphere formation was inhibited by 3- to 5-fold in both MDA-MB-231 and SUM159 cells when treated with PF-573228 in a concentration-dependent manner (Fig 5B). To investigate the role of mTOR signaling in BCSC function, we treated SUM159 and MDA-MB-231 cells with FDA approved mTOR inhibitor everolimus and found that everolimus inhibited soft-agar colony formation 10-to 15-fold compared to untreated cells in a concentration dependent manner in both cell types (Fig 5B). Together, these data indicate that signaling pathways downstream of FAK and mTOR regulate BCSC function in TNBC cells.

Knockout of ST8SIA1 inhibits tumorigenesis and metastases in vivo

Finally, to investigate the effects of ST8SIA1inhibition on *in vivo* tumor growth, Cas9-Control or ST8SIA1-KO SUM159 cells (3×10^6 per mouse) were implanted into the mammary fat pads of NSG mice and tumor growth monitored weekly. The experiment was terminated when the control tumors reached ~2 cm in diameter as per institutional IACUC regulations. Control tumors reached 2 cm in diameter within 4–5 weeks after implantation, whereas no tumor growth was observed in mice implanted with ST8SIA1-KO cells, even 10

weeks after implantation (Fig 6A). In the mice implanted with ST8SIA1-KO cells, surgical dissection found only the matrigel plug that was implanted at the site of injection (Fig 6B). Histologic analysis revealed typical xenograft tumor histology in the control tumors but only a few randomly dispersed cells in matrigel derived from ST8SIA1-KO cells (Fig 6C). Cas9-Control–implanted mice were dead by day 40 (n=10), whereas 100% of the ST8SIA1-KO–implanted mice survived at least 100 days after tumor cell implantation (n=7; Fig 6D). These data suggest that the ST8SIA1-KO cells lost their ability to initiate tumors *in vivo*.

To investigate whether ST8SIA1 regulates TNBC metastasis, NSG mice were injected in the tail vein with Cas9-Control or ST8SIA1-KO SUM159 cells (5×10^5 per mouse). Beginning at week 3, three mice were sacrificed weekly, and their lungs were isolated, fixed in formalin, and embedded in paraffin for histologic studies. The H&E-stained sections showed distinct lung metastasis in the mice injected with the control SUM159 cells 4 weeks after implantation. In contrast, the lungs of mice injected with KO cells were completely free of metastases even after week 5 (Figs 6E and6F). These data suggest that ST8SIA1 regulates tumor growth and metastasis and is a potential therapeutic target in TNBC.

Discussion

In this report, we conclude that ST8SIA1 is a potential target in TNBC and that inhibition of this enzyme will reduce tumor growth and metastasis by eliminating $GD2^+$ BCSCs. ST8SIA1 is highly upregulated in basal-like TNBC cell lines and patient samples compared to other breast cancer sub-types. In addition, ST8SIA1 is a prognostic factor in TNBC and its expression is highly correlated with the presence of p53 mutations. ST8SIA1 expression is positively correlated with genes that are closely associated with BCSCs. Knockout of ST8SIA1 dramatically reduced *in vitro* tumorigenesis and mammosphere formation and completely eradicated tumor growth and metastasis *in vivo*. In mechanistic studies, knockout of ST8SIA expression reduced activation of several oncogenic pathways, including RAS, AKT, and MAPK. Proteomics analysis revealed that FAK and its downstream signaling are highly active in $GD2^+$ BCSCs and that this activity is highly dependent on ST8SIA1. Knockout of ST8SIA1 inhibited FAK-AKT-ERK-mTOR signaling, suggesting that ST8SIA1-regulated stem cell activity is mediated through this pathway.

Although ST8SIA1 is not directly involved in the biosynthesis of GD2, it is highly upregulated in $GD2^+$ BCSCs. ST8SIA1 is the key enzyme in the biosynthesis of b- and c-series gangliosides, including GD3, GD2, GD1b, GT1b, and GQ1b in the b-series and GT3, GT2, GT1c, GQ1c and GP1c. Among these gangliosides, GD3 and GD2 are known to be upregulated in several different cancer types, including malignant melanoma (30, 31), neuroblastoma (32), glioma (33, 34), small cell lung cancer (35), and osteosarcoma (12, 36). However, only a few normal tissues, such as brain and skin, express these gangliosides. Our data suggest that ST8SIA1 is highly upregulated in basal-like cell breast cancers compared to the luminal types. It is interesting to note that GD2 expression in BCSCs is also associated mostly with basal-like cell lines, further indicating the association between ST8SIA1 and GD2. Analysis of TCGA data suggests that ST8SIA1 is overexpressed in breast tumors with the ER negative and PR negative phenotype. In addition, ST8SIA1 expression was 4.6-fold higher in TNBC than in non-TNBC breast cancer types.

Furthermore, the mesenchymal subtype of TNBC has the highest ST8SIA1 expression of all subtypes. These findings are particularly interesting because the mesenchymal subtype is one of the most aggressive subtypes of TNBC, with the lowest overall survival amongst all TNBC subtypes (37). Although the role of ST8SIA1 in normal stem cells is not clear, ST8SIA1 knockout was found not to affect behavior, total life span, or reproductive capacity in mice(38, 39). These data suggest that loss of ST8SIA1 may not affect normal stem cells but may be deleterious for cancer stem cells, making ST8SIA1 an ideal target for inhibiting BCSC function in TNBC. These data suggest that ST8SIA1 expression is a specific marker for TNBC and could potentially be a therapeutic target in these cancers.

The high correlation between ST8SIA1 expression and mutations in the TP53 gene is another indication that ST8SIA1 is associated with the TNBC subtype, as over 80% of TNBC tumors have a mutation in this gene. Recent data suggest that mutations in TP53 disrupt mammary tissue architecture and are associated with a cancer stem cell phenotype (40, 41). Considering that mutations in the TP53 gene because many different types of cancer, ST8SIA1 could be a novel downstream target of mutated TP53 that supports oncogenic potential. In addition, ST8SIA1 expression is positively correlated with genes that are associated with BCSC function, including BCL11A, FOXC1, CXCR4, CXCL12, and VGLL1, suggesting the tumorigenic nature of cells expressing ST8SIA1. These observations further support our finding that ST8SIA1 is associated with BCSCs in TNBC tumors.

Knockout of ST8SIA1 completely blocked BCSC function, including anchorage-independent growth, mammosphere formation, and migration *in vitro*. In addition, knockout of ST8SIA1 completely inhibited tumor initiation and metastasis, which are characteristic features of BCSCs. These data support ST8SIA1 as a major target in TNBC and suggest that inhibitors targeting this enzyme could have high therapeutic potential in TNBC expressing ST8SIA1. Our findings suggest that the mechanism of ST8SIA1-mediated regulation of BCSCs involves the regulation of several genes associated with cancer progression and, more importantly, BCSC function. These genes include BCL11A, PDGFRβ, VCAM1, PDGFRα, SOX2, FOXC1, CXCR4, CXCL12, and FGFR2. BCL11A and FOXC1 have been reported to be upregulated in BCSCs and to regulate their function (25, 27). We have previously shown that induction of EMT enhances PDGFRβ expression in breast epithelial cells (42). Considering that EMT induces the stem cell phenotype in breast cancer cells (43), ST8SIA1 regulation of PDGFRβ suggests that this receptor has a role in the regulation of BCSC function. SOX2 and VCAM1 are other important proteins implicated in maintenance of BCSC function that are regulated by ST8SIA1 (44, 45). We reported that CXCR4, the receptor for CXCL12, has a crucial role in the regulation of breast cancer metastasis (46). GSEA analysis of the genes differentially regulated in ST8SIA1-KO and control cells suggests that several signaling pathways that regulate cell survival, proliferation, and migration, including AKT, ERK, RAS, p53, EGFR, and PDGF, are downregulated in the absence of ST8SIA1 in TNBC. These findings indicate that ST8SIA1 regulates BCSC function by regulating expression of several oncogenes involved in tumor growth and metastasis.

GD2 has been shown to interact with cell surface receptors and to activate signaling downstream in several cancer types (8). We are currently developing a clinical protocol to

target $GD2^+$ BCSCs using the FDA approved chimeric anti-GD2 monoclonal antibody (Dinutuximab®) in patients with TNBC. Our proteomics finding that FAK and mTOR signaling is activated in $GD2^+$ compared to $GD2^-$ cells, along with further analysis, provides important clues about downstream signal transducers associated with this signaling pathways. AKT and ERK, key proteins in the regulation of cell survival and proliferation, are highly upregulated in $GD2^+$ TNBC cells compared to $GD2^-$ cells. In addition, phosphorylation of these proteins was inhibited by ST8SIA1 knockout, suggesting that ST8SIA1 regulates activation of these signaling proteins in TNBC cells. Furthermore, we found that 4E-BP1, a downstream target of the mTORC1 complex, is highly phosphorylated in $GD2^+$ cells. Western blot analysis confirmed downregulation of phosphorylated mTOR and 4E-BP1 in ST8SIA1-KO cells. Thus our data demonstrate, for the first time, that ST8SIA1 regulates the FAK-AKT-ERK-mTOR signaling pathway in BCSCs.

In conclusion, our findings elucidate some of the mechanisms by which ST8SIA1 inhibition could suppress tumor growth/initiation and metastasis in TNBC. Targeting ST8SIA1 could be future therapeutic strategy that could reduce cancer recurrence and extend survival in TNBC patients.

Supplementary Material

Refer to Web version on PubMed Central for supplementary material.

Acknowledgements

The authors thank Dr. Arvind Rao at MD Anderson Cancer Center for his suggestions concerning the TCGA data analysis.

Support: This work is supported by grants from the Breast Cancer Research Foundation (BCRF), the MD Anderson Cancer Center Support Grant (CA016672), and the Paul and Mary Haas Chair in Genetics (to MA), and by the Berdon Lawrence Research Award from Bone Disease Program of Texas (to VLB).

References

1. Gangopadhyay S, Nandy A, Hor P, Mukhopadhyay A. Breast cancer stem cells: a novel therapeutic target. Clin Breast Cancer. 2013;13:7–15. [PubMed: 23127340]
2. Geng SQ, Alexandrou AT, Li JJ. Breast cancer stem cells: Multiple capacities in tumor metastasis. Cancer Lett. 2014;349:1–7. [PubMed: 24727284]
3. Stratford AL, Reipas K, Maxwell C, Dunn SE. Targeting tumour-initiating cells to improve the cure rates for triple-negative breast cancer. Expert Rev Mol Med. 2010;12:e22. [PubMed: 20653987]
4. Al-Hajj M, Wicha MS, Benito-Hernandez A, Morrison SJ, Clarke MF. Prospective identification of tumorigenic breast cancer cells. Proc Natl Acad Sci U S A. 2003;100:3983–8. [PubMed: 12629218]
5. Ginestier C, Hur MH, Charafe-Jauffret E, Monville F, Dutcher J, Brown M, et al. ALDH1 is a marker of normal and malignant human mammary stem cells and a predictor of poor clinical outcome. Cell Stem Cell. 2007;1:555–67. [PubMed: 18371393]
6. Battula VL, Shi Y, Evans KW, Wang RY, Spaeth EL, Jacamo RO, et al. Ganglioside GD2 identifies breast cancer stem cells and promotes tumorigenesis. J Clin Invest. 2012;122:2066–78. [PubMed: 22585577]
7. Liang YJ, Ding Y, Levery SB, Lobaton M, Handa K, Hakomori SI. Differential expression profiles of glycosphingolipids in human breast cancer stem cells vs. cancer non-stem cells. Proc Natl Acad Sci U S A. 2013;110:4968–73. [PubMed: 23479608]

8. Liang YJ, Wang CY, Wang IA, Chen YW, Li LT, Lin CY, et al. Interaction of glycosphingolipids GD3 and GD2 with growth factor receptors maintains breast cancer stem cell phenotype. Oncotarget. 2017;8:47454–73. [PubMed: 28537895]
9. Sarkar TR, Battula VL, Werden SJ, Vijay GV, Ramirez-Pena EQ, Taube JH, et al. GD3 synthase regulates epithelial-mesenchymal transition and metastasis in breast cancer. Oncogene. 2015;34:2958–67. [PubMed: 25109336]
10. Battula VL, Nguyen K, Sun J, Pitner MK, Yuan B, Bartholomeusz C, et al. IKK inhibition by BMS-345541 suppresses breast tumorigenesis and metastases by targeting GD2+ cancer stem cells. Oncotarget. 2017;8:36936–49. [PubMed: 28415808]
11. Luo M, Guan JL. Focal adhesion kinase: a prominent determinant in breast cancer initiation, progression and metastasis. Cancer Lett. 2010;289:127–39. [PubMed: 19643531]
12. Shibuya H, Hamamura K, Hotta H, Matsumoto Y, Nishida Y, Hattori H, et al. Enhancement of malignant properties of human osteosarcoma cells with disialyl gangliosides GD2/GD3. Cancer Sci. 2012;103:1656–64. [PubMed: 22632091]
13. Guan JL. Integrin signaling through FAK in the regulation of mammary stem cells and breast cancer. IUBMB Life. 2010;62:268–76. [PubMed: 20101634]
14. Cazet A, Bobowski M, Rombouts Y, Lefebvre J, Steenackers A, Popa I, et al. The ganglioside G(D2) induces the constitutive activation of c-Met in MDA-MB-231 breast cancer cells expressing the G(D3) synthase. Glycobiology. 2012;22:806–16. [PubMed: 22301273]
15. Cary LA, Guan JL. Focal adhesion kinase in integrin-mediated signaling. Front Biosci. 1999;4:D102–13. [PubMed: 9889179]
16. Xia H, Nho RS, Kahm J, Kleidon J, Henke CA. Focal adhesion kinase is upstream of phosphatidylinositol 3-kinase/Akt in regulating fibroblast survival in response to contraction of type I collagen matrices via a beta 1 integrin viability signaling pathway. J Biol Chem. 2004;279:33024–34. [PubMed: 15166238]
17. Jindra PT, Jin YP, Rozengurt E, Reed EF. HLA class I antibody-mediated endothelial cell proliferation via the mTOR pathway. J Immunol. 2008;180:2357–66. [PubMed: 18250445]
18. Schlaepfer DD, Hunter T. Focal adhesion kinase overexpression enhances ras-dependent integrin signaling to ERK2/mitogen-activated protein kinase through interactions with and activation of c-Src. J Biol Chem. 1997;272:13189–95. [PubMed: 9148935]
19. You D, Xin J, Volk A, Wei W, Schmidt R, Scurti G, et al. FAK mediates a compensatory survival signal parallel to PI3K-AKT in PTEN-null T-ALL cells. Cell Rep. 2015;10:2055–68. [PubMed: 25801032]
20. Carter BZ, Mak PY, Wang X, Yang H, Garcia-Manero G, Mak DH, et al. Focal Adhesion Kinase as a Potential Target in AML and MDS. Mol Cancer Ther. 2017;16:1133–44. [PubMed: 28270436]
21. Slack-Davis JK, Martin KH, Tilghman RW, Iwanicki M, Ung EJ, Autry C, et al. Cellular characterization of a novel focal adhesion kinase inhibitor. J Biol Chem. 2007;282:14845–52. [PubMed: 17395594]
22. Langmead B, Salzberg SL. Fast gapped-read alignment with Bowtie 2. Nature methods. 2012;9:357–9. [PubMed: 22388286]
23. Li B, Dewey CN. RSEM: accurate transcript quantification from RNA-Seq data with or without a reference genome. BMC bioinformatics. 2011;12:323. [PubMed: 21816040]
24. Robinson MD, McCarthy DJ, Smyth GK. edgeR: a Bioconductor package for differential expression analysis of digital gene expression data. Bioinformatics. 2010;26:139–40. [PubMed: 19910308]
25. Khaled WT, Choon Lee S, Stingl J, Chen X, Raza Ali H, Rueda OM, et al. BCL11A is a triple-negative breast cancer gene with critical functions in stem and progenitor cells. Nat Commun. 2015;6:5987. [PubMed: 25574598]
26. Han B, Bhowmick N, Qu Y, Chung S, Giuliano AE, Cui X. FOXC1: an emerging marker and therapeutic target for cancer. Oncogene. 2017;36:3957–63. [PubMed: 28288141]
27. Han B, Qu Y, Yu-Rice Y, Johnson J, Cui X. FOXC1-induced Gli2 activation: A non-canonical pathway contributing to stemness and anti-Hedgehog resistance in basal-like breast cancer. Mol Cell Oncol. 2016;3:e1131668. [PubMed: 27314088]

28. Chu IM, Lai WC, Aprelikova O, El Touny LH, Kouros-Mehr H, Green JE. Expression of GATA3 in MDA-MB-231 triple-negative breast cancer cells induces a growth inhibitory response to TGFss. PLoS One. 2013;8:e61125. [PubMed: 23577196]
29. Hisamatsu Y, Tokunaga E, Yamashita N, Akiyoshi S, Okada S, Nakashima Y, et al. Impact of GATA-3 and FOXA1 expression in patients with hormone receptor-positive/HER2-negative breast cancer. Breast Cancer. 2015;22:520–8. [PubMed: 24415069]
30. Lloyd KO, Old LJ. Human monoclonal antibodies to glycolipids and other carbohydrate antigens: dissection of the humoral immune response in cancer patients. Cancer Res. 1989;49:3445–51. [PubMed: 2471585]
31. Hamamura K, Furukawa K, Hayashi T, Hattori T, Nakano J, Nakashima H, et al. Ganglioside GD3 promotes cell growth and invasion through p130Cas and paxillin in malignant melanoma cells. Proc Natl Acad Sci U S A. 2005;102:11041–6. [PubMed: 16040804]
32. Schengrund CL, Shochat SJ. Gangliosides in neuroblastomas. Neurochem Pathol. 1988;8:189–202. [PubMed: 3075728]
33. Fredman P, von Holst H, Collins VP, Ammar A, Dellheden B, Wahren B, et al. Potential ganglioside antigens associated with human gliomas. Neurol Res. 1986;8:123–6. [PubMed: 2875407]
34. Wikstrand CJ, Fredman P, Svennerholm L, Bigner DD. Detection of glioma-associated gangliosides GM2, GD2, GD3, 3'-isoLM1 3',6'-isoLD1 in central nervous system tumors in vitro and in vivo using epitope-defined monoclonal antibodies. Prog Brain Res. 1994;101:213–23. [PubMed: 7518092]
35. Yoshida S, Fukumoto S, Kawaguchi H, Sato S, Ueda R, Furukawa K. Ganglioside G(D2) in small cell lung cancer cell lines: enhancement of cell proliferation and mediation of apoptosis. Cancer Res. 2001;61:4244–52. [PubMed: 11358851]
36. Heiner JP, Miraldi F, Kallick S, Makley J, Neely J, Smith-Mensah WH, et al. Localization of GD2-specific monoclonal antibody 3F8 in human osteosarcoma. Cancer Res. 1987;47:5377–81. [PubMed: 3115567]
37. Lehmann BD, Bauer JA, Chen X, Sanders ME, Chakravarthy AB, Shyr Y, et al. Identification of human triple-negative breast cancer subtypes and preclinical models for selection of targeted therapies. J Clin Invest. 2011;121:2750–67. [PubMed: 21633166]
38. Okada M, Itoh Mi M, Haraguchi M, Okajima T, Inoue M, Oishi H, et al. b-series Ganglioside deficiency exhibits no definite changes in the neurogenesis and the sensitivity to Fas-mediated apoptosis but impairs regeneration of the lesioned hypoglossal nerve. J Biol Chem. 2002;277:1633–6. [PubMed: 11682464]
39. Bernardo A, Harrison FE, McCord M, Zhao J, Bruchey A, Davies SS, et al. Elimination of GD3 synthase improves memory and reduces amyloid-beta plaque load in transgenic mice. Neurobiol Aging. 2009;30:1777–91. [PubMed: 18258340]
40. Cicalese A, Bonizzi G, Pasi CE, Faretta M, Ronzoni S, Giulini B, et al. The tumor suppressor p53 regulates polarity of self-renewing divisions in mammary stem cells. Cell. 2009;138:1083–95. [PubMed: 19766563]
41. Spike BT, Wahl GM. p53, Stem Cells, and Reprogramming: Tumor Suppression beyond Guarding the Genome. Genes Cancer. 2011;2:404–19. [PubMed: 21779509]
42. Battula VL, Evans KW, Hollier BG, Shi Y, Marini FC, Ayyanan A, et al. Epithelial-mesenchymal transition-derived cells exhibit multilineage differentiation potential similar to mesenchymal stem cells. Stem Cells. 2010;28:1435–45. [PubMed: 20572012]
43. Mani SA, Guo W, Liao MJ, Eaton EN, Ayyanan A, Zhou AY, et al. The epithelial-mesenchymal transition generates cells with properties of stem cells. Cell. 2008;133:704–15. [PubMed: 18485877]
44. Mukherjee P, Gupta A, Chattopadhyay D, Chatterji U. Modulation of SOX2 expression delineates an end-point for paclitaxel-effectiveness in breast cancer stem cells. Sci Rep. 2017;7:9170. [PubMed: 28835684]
45. Wang PC, Weng CC, Hou YS, Jian SF, Fang KT, Hou MF, et al. Activation of VCAM-1 and its associated molecule CD44 leads to increased malignant potential of breast cancer cells. Int J Mol Sci. 2014;15:3560–79. [PubMed: 24583847]

46. Ling X, Spaeth E, Chen Y, Shi Y, Zhang W, Schober W, et al. The CXCR4 antagonist AMD3465 regulates oncogenic signaling and invasiveness in vitro and prevents breast cancer growth and metastasis in vivo. PLoS One. 2013;8:e58426. [PubMed: 23484027]

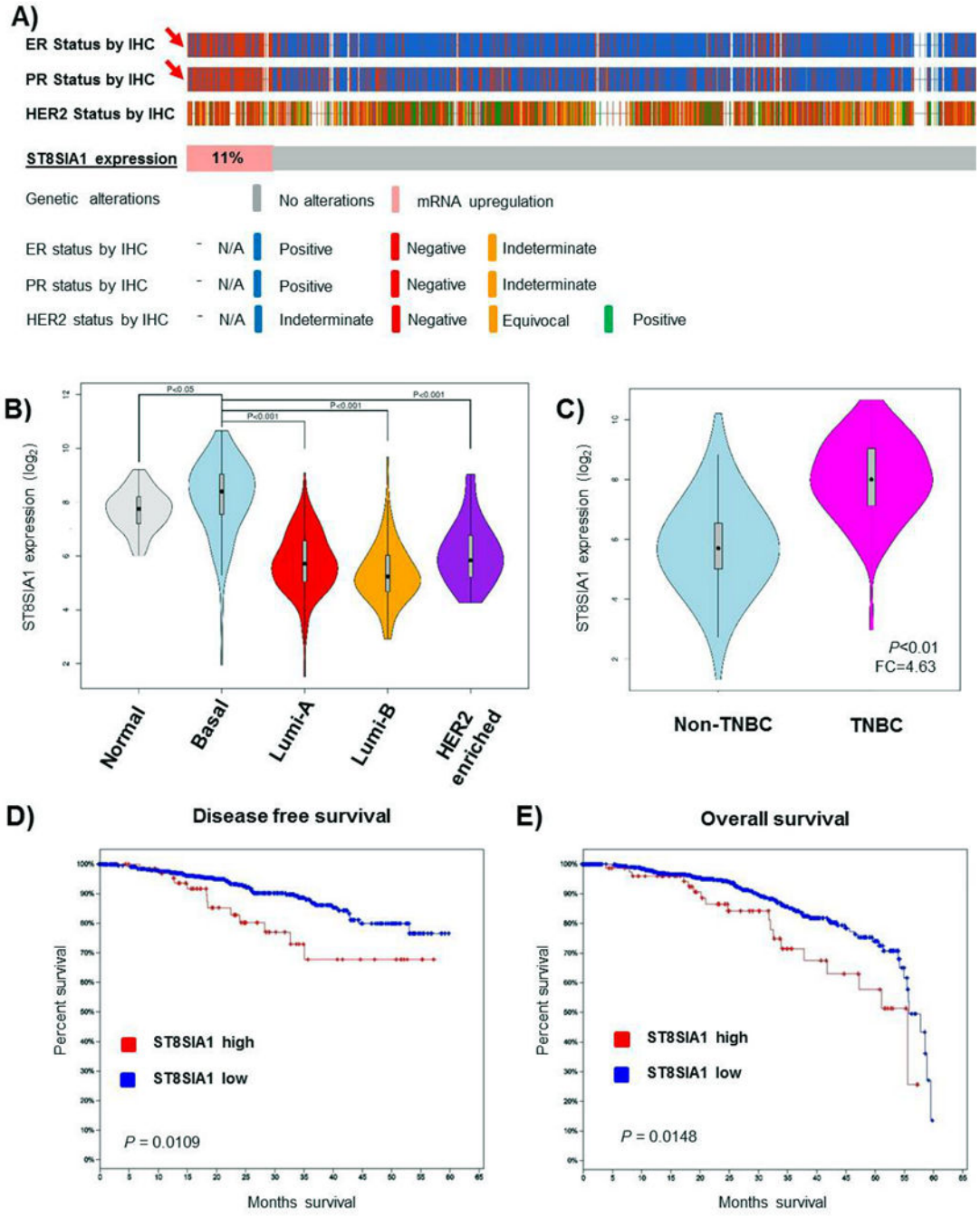

Figure 1.

ST8SIA1 expression in primary TNBC tumors is associated primarily with the basal-like subtype. **(A)** ST8SIA1 expression was analyzed in primary tumors using RNA sequencing data derived from the TCGA breast cancer data set (n=1093). Absence of expression of hormone receptors (estrogen receptor [ER] and progesterone receptor [PR]) and HER2 (determined by immunohistochemistry [IHC]) in primary tumors was correlated with ST8SIA1 overexpression. Receptor expression status is indicated in different colors. The figure was generated by using the cBioportal web tool. (**B)** Comparative analysis of

ST8SIA1 expression in different breast cancer subtypes, including basal, luminal A, luminal B, and HER2-enriched, and normal breast tissue. (**C**) ST8SIA1 expression in primary TNBC vs non-TNBC tumors. FC, fold-change. **(D,E)** Disease-free and Overall survival analysis for a 60-month follow-up period of breast cancer patients with high or low ST8SIA1 expression. Data were analyzed and figures generated by statistical program R. Statistical significance for each analysis is indicated in the figure in the form of p-value.

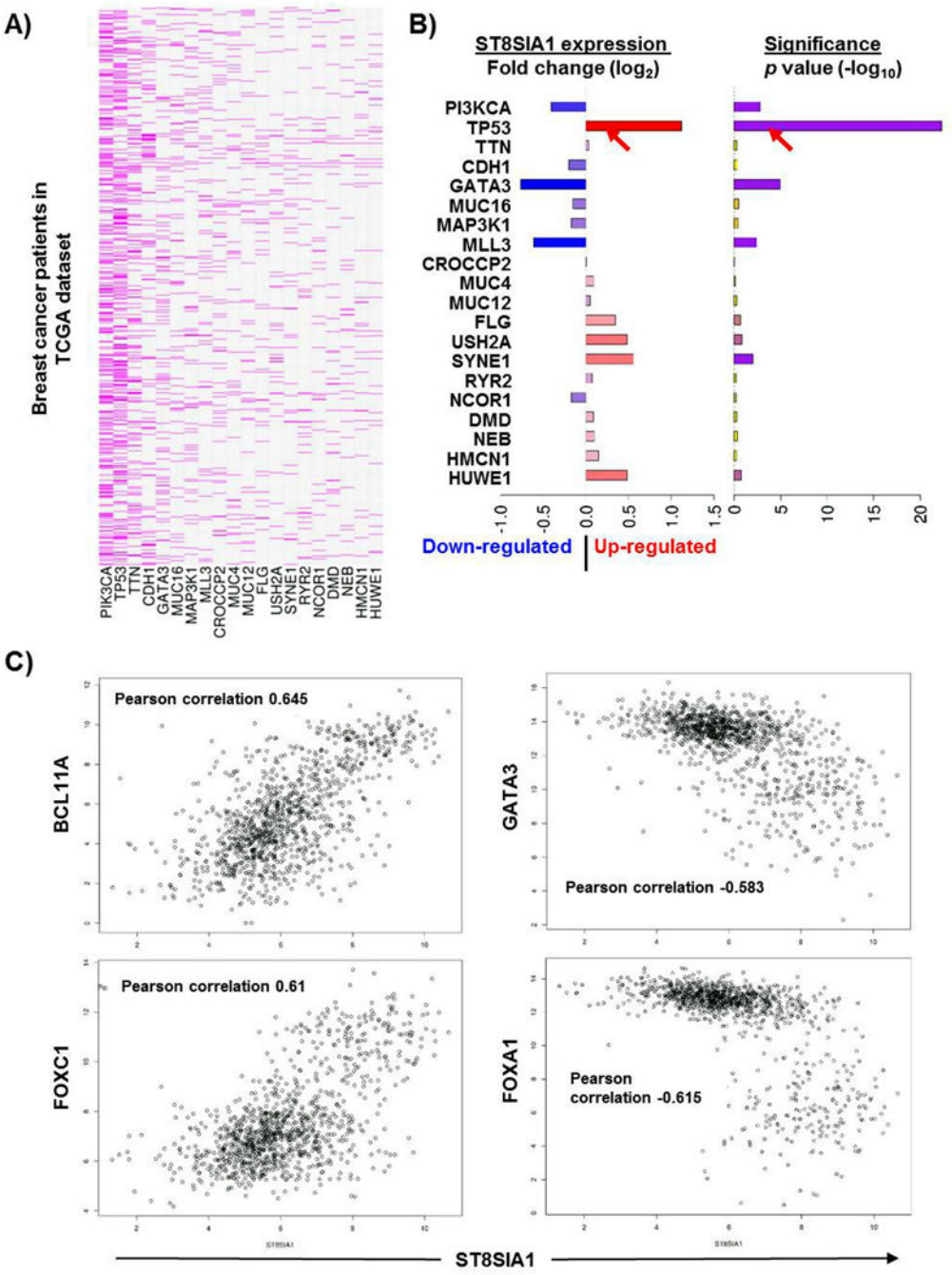

Figure 2.

ST8SIA1 is overexpressed in breast tumors with mutations in the TP53 gene and is highly correlated with a BCSC–associated gene signature. (**A**) The 20 most frequent gene mutations in breast cancers, as determined from the TCGA breast cancer data set. The mutations are ranked from left to right based on their frequency. (**B**) (Left) ST8SIA1 mRNA expression was analyzed in primary tumors with one of the mutations listed in (A). Upregulation of ST8SIA1 is represented by the red gradient and downregulation by the blue gradient. (Right) The statistical significance of ST8SIA1 expression level for each mutation.

(**C**) Correlation analysis of ST8SIA1 expression with expression of BCL11A and FOXC1 (positive) and GATA3 and FOXA1 (negative). The correlation analysis was performed using the R statistical analysis tool.

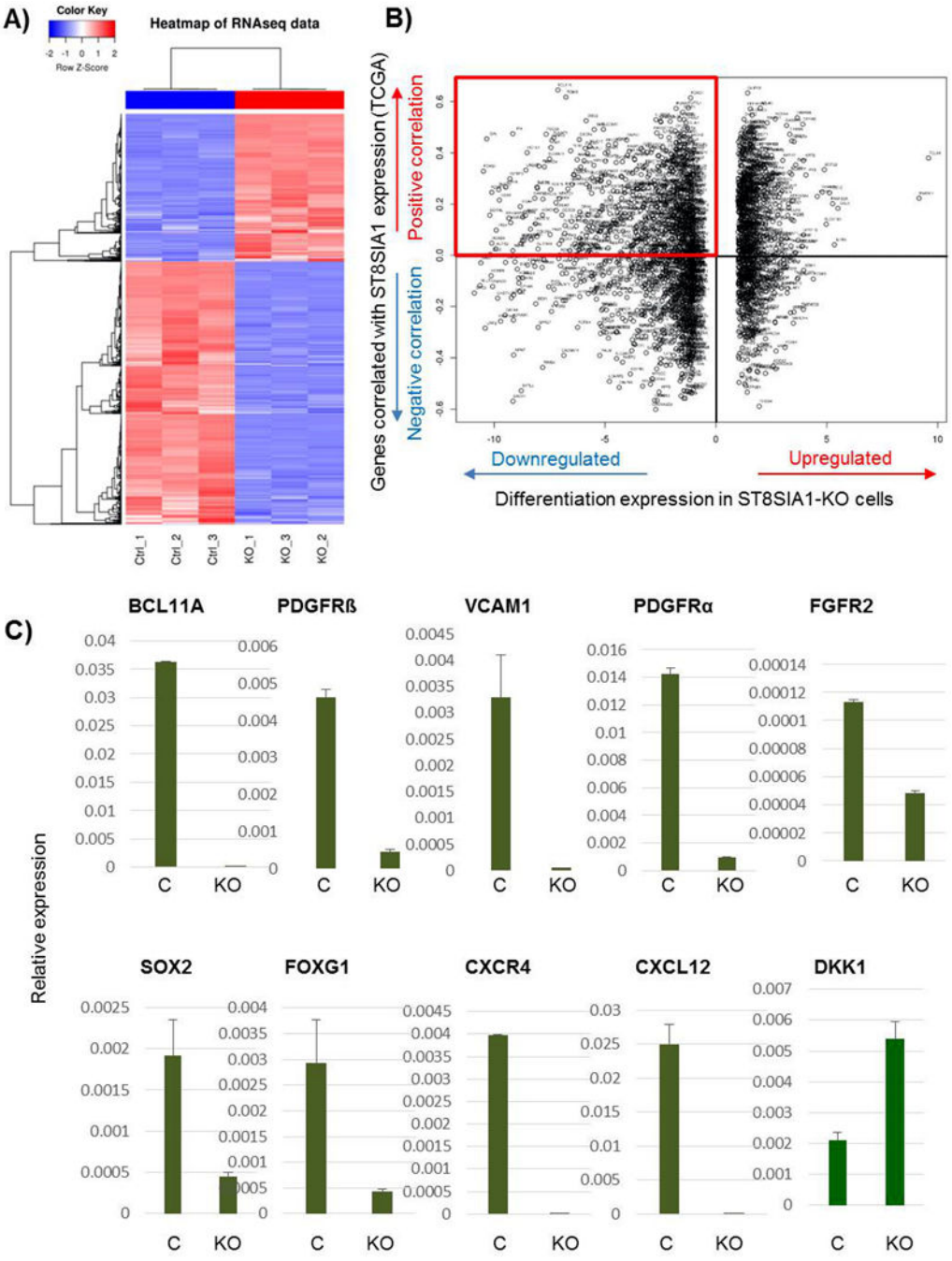

Figure 3.

Expression of genes associated with BCSC function is dependent on ST8SIA1. (**A**) RNA sequencing analysis (RNAseq) was performed on Cas9-Control and ST8SIA1-knockout (ST8SIA1-KO) SUM159 cells. Data were analyzed and the results clustered by using R statistical software. Blue bars indicate downregulated genes and red bars indicate upregulated genes. (**B**) Correlative analysis between genes that were positively or negatively correlated with ST8SIA1 in the TCGA data set and genes that were upregulated or downregulated by ST8SIA1 knockout in SUM159 cells. Pearson correlation coefficients

were used to denote the correlation between ST8SIA1 and other genes in TCGA data (y axis) and differential gene expression in ST8SIA1-KO compared to Cas9-control cells (x axis, fold change in $\log_2$). In the top left corner are genes that were positively correlated with ST8SIA1 and downregulated upon ST8SIA1 knockout, indicating that their expression is dependent on ST8SIA1 expression. (**C**) mRNA expression of some of the genes found in the red box in (B) was analyzed in Cas9-Control and ST8SIA1-KO SUM159 cells by qRT-PCR analysis. Differential expression of all the genes tested in ST8SIA1-KO cells is significant ($p<0.001$).

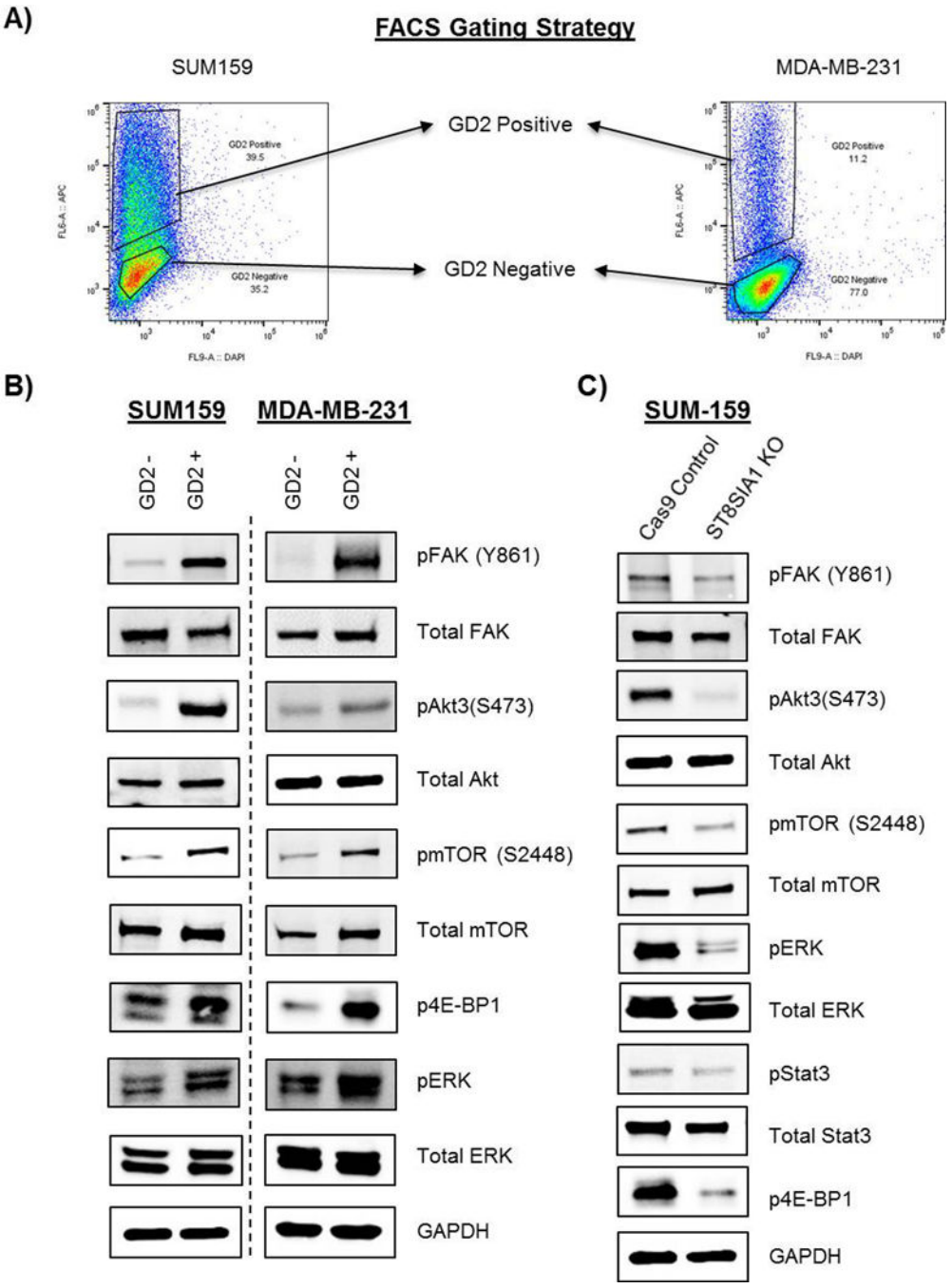

Figure 4.

FAK-AKT-ERK-mTOR signaling is activated in GD2^{+} TNBC cells and its activation is dependent on ST8SIA1 expression. (**A**) GD2^{+} and GD2^{-} cells were sorted by fluorescence-activated cell sorting (FACS) from SUM159 or MDA-MB-231 cells per the gating strategy shown. (**B**) Lysates of FACS-sorted cells (A) were analyzed by western blot (IB). The membranes were incubated with primary antibodies as shown. The membranes were then incubated with fluorochrome-conjugated secondary antibodies and scanned on an Odyssey fluorescent imager. (**C**) Lysates from Cas9-Control or ST8SIA1-knockout (ST8SIA1-KO)

SUM159 cells were subjected to western 5blot analysis using total- and phospho-protein specific antibodies as shown. The results were normalized to GAPDH expression.

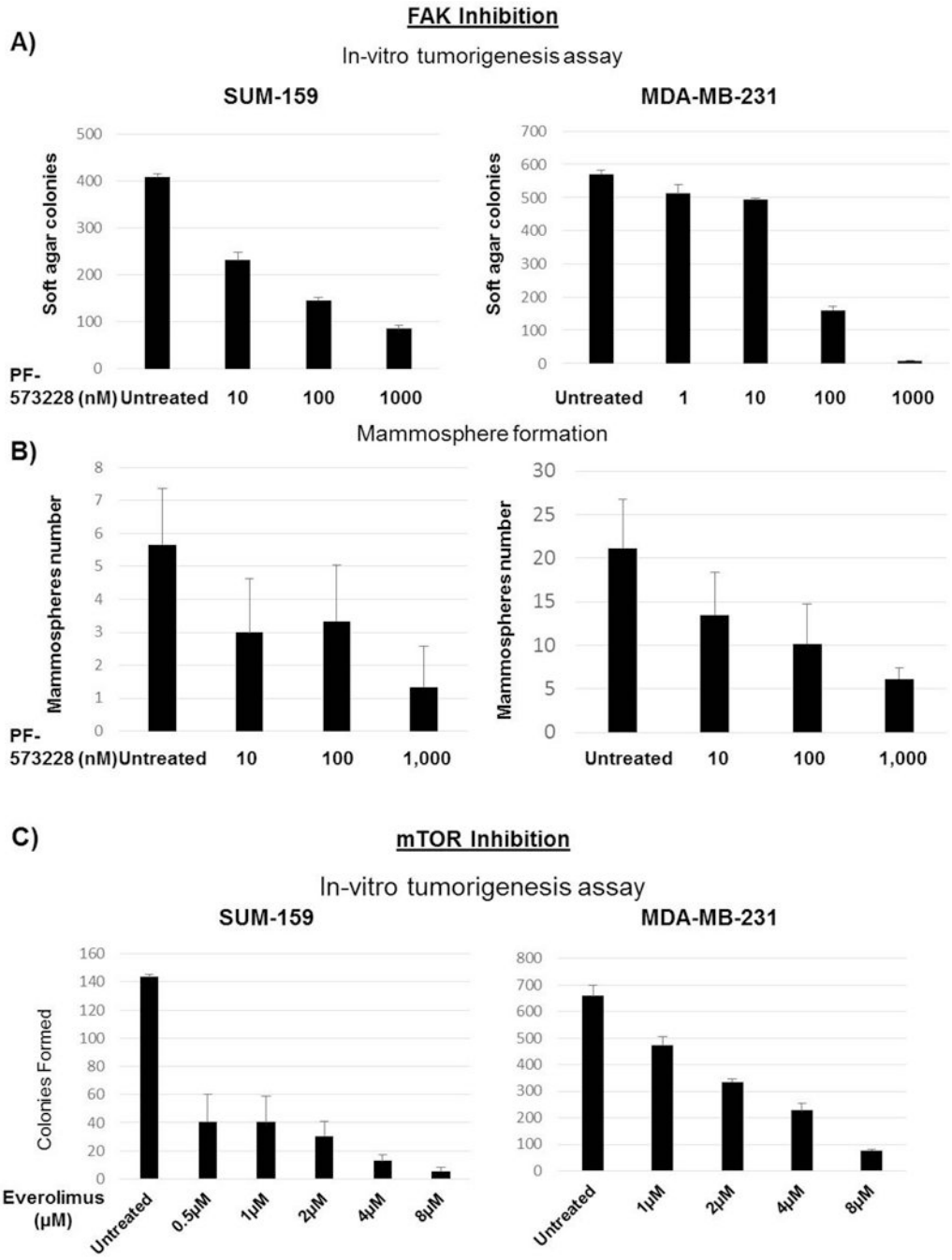

Figure 5.

Inhibition of FAK or mTOR signaling targets BCSC function. **(A)** 5×10^3 SUM159 or MDA-MB-231 cells were seeded into soft agar containing different concentrations of a FAK inhibitor, PF-573228. After 3 weeks, the colonies were fixed and stained by the MTT method. Tumorigenesis was assessed by counting the resulting colonies by an automated colony counter. (**B**) SUM159 or MDA-MB-231 cells were seeded (1×10^3 per well) into low-adherent dishes containing mammocult medium with different concentrations of PF-573228. After 3 weeks, the mammospheres were stained with MTT reagent and counted by an

automated colony counter. (**C)** SUM159 or MDA-MB-231 cells were seeded (5×10^3 per well) into soft agar containing different concentrations of mTOR inhibitor everolimus. After 3 weeks, the colonies were stained and counted as for (A). All the experiments were performed in triplicate for each drug concentration.

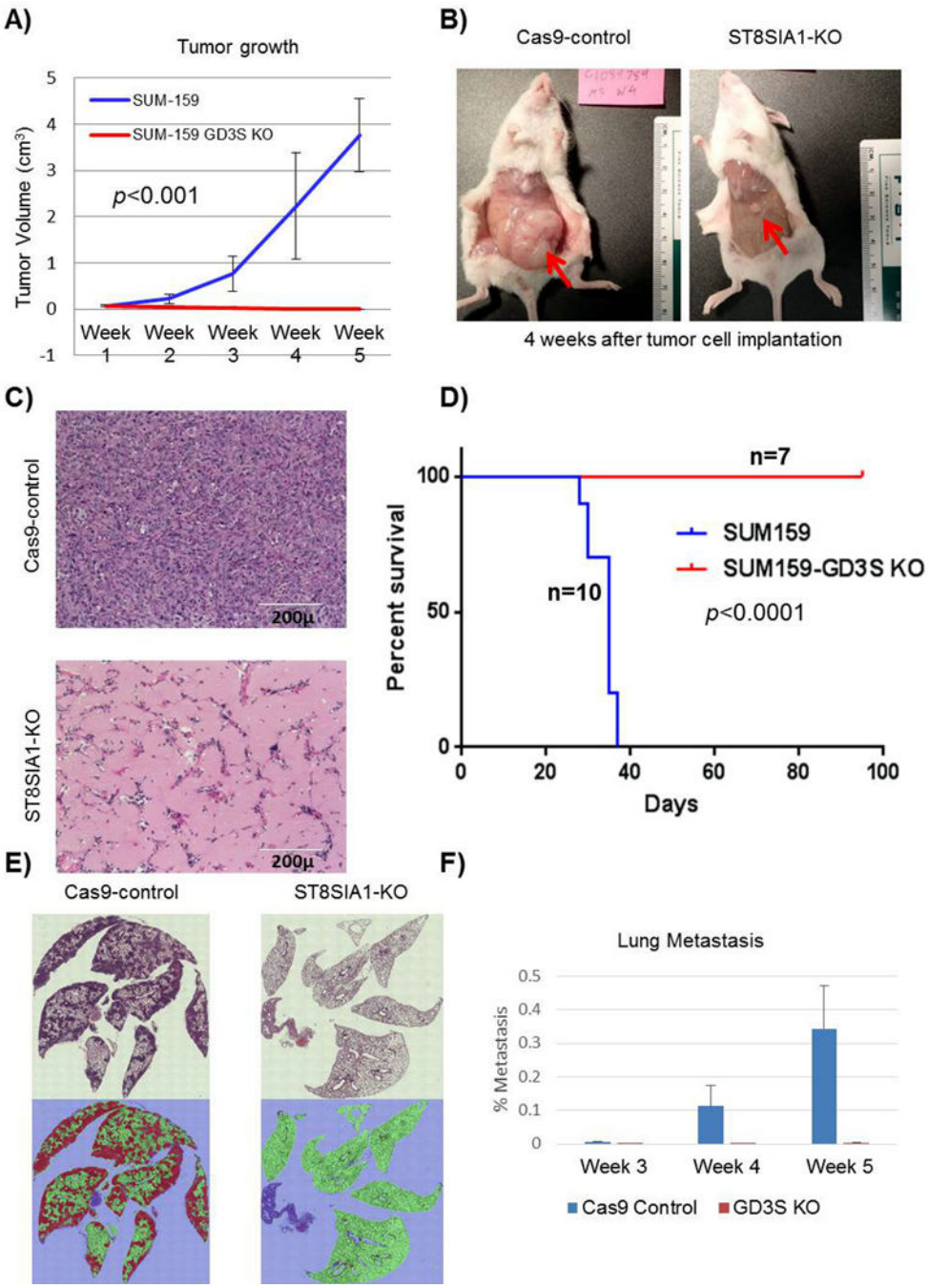

Figure 6.

Knockout of ST8SIA1 halts TNBC tumor initiation and metastasis *in vivo*. **(A)** Cas9-Control or ST8SIA1-knockout (ST8SIA1-KO) SUM159 cells were implanted (3×10^3 per mouse) into the mammary fat pads of NSG mice (n=20, 10 mice per group). Tumor volumes were measured weekly. (**B**) Starting at week 3, three mice chosen randomly from each of the two groups were sacrificed weekly for tumor visualization. Representative mice from each group at 4 weeks are shown. (**C**) Formalin-fixed and paraffin-embedded tumors derived from Cas9-Control or ST8SIA1-KO SUM159 cells were stained with hematoxylin and eosin (H&E) for

histologic examination. A representative tumor from each group is shown (scale bar=200 microns). (**D)** Survival analysis of mice implanted with Cas9-Control or ST8SIA1-KO SUM159 cells by log-rank test. (**E**) Cas9-Control or ST8SIA1-KO MDA-MB-231 cells were injected (5×10^5 per mouse) into the tail veins of NSG mice (n=18, 9 mice per group). Starting at week 3, three randomly chosen mice from each group were sacrificed weekly for organ harvest. Lung tissues from both groups of mice were formalin-fixed, paraffin-embedded, and stained with H&E. Images were taken on a light microscope and metastasis was quantified using analysis software. A representative tumor from each group is shown. The upper images show the original H&E staining, and the lower images show the software-enhanced image with distinct metastatic colonies in red. (**F)** Quantitative representation of lung metastasis observed in (E).